Materials Advances

ROYAL SOCIETY OF CHEMISTRY

PAPER

View Article Online
View Journal

Cite this: DOI: 10.1039/d5ma01477h

Experimental assessment of lime-based mortars modified with eggshell powder and egg white – towards development of materials for repair of historic buildings

Zbyšek Pavlík, *[a] Adam Pivák,[a] Martina Záleská, [a] Grzegorz Łagód,[b] Milena Pavlíková[a] and Ondřej Jankovský[c]

In this paper, mechanically processed eggshells were employed as a partial replacement for silica sand in lime-based mortars intended for the repair of historic buildings. To ensure the workability of fresh mortar mixes on the control value, egg white was incorporated as a natural modifying agent. The introduction of these organic constituents aligns with current conservation and repair approaches, which prioritize material compatibility, reduced environmental impact, and a return to historically validated construction practices. The study evaluates the influence of ground eggshells and egg white on the fresh and hardened properties of the mortars, with particular emphasis on their mechanical performance, pore structure, thermal and hygric performance, and potential applicability in heritage conservation. Higher substitution ratios of fine silica sand with eggshell powder, namely 50 vol% and 75 vol%, made it possible to produce mortars with increased porosity, adequate mechanical strength, and high water vapour permeability, making them suitable for conservation and repair of historical masonry. The addition of egg white helped maintain the desired workability of fresh mortars. Moreover, it reduced water ingress by forming a hydrophobic layer of denatured proteins within the pore structure, which may consequently improve the mortars' resistance to moisture-related deterioration processes.

Received 17th December 2025,
Accepted 11th February 2026

DOI: 10.1039/d5ma01477h

rsc.li/materials-advances

Introduction

Lime-based mortars were the primary building material from ancient times until the late 19th century, when it was largely replaced by Portland cement.[1,2] Due to their compatibility, breathability, flexibility and sustainability, they have experienced and revival in modern conservation of historic buildings.[3,4] Historically, mortar composition was far from standardized. While lime (the binder) and an inorganic aggregate (typically sand) formed the basic matrix, the true "recipe" was often site- specific, incorporating a wide array of organic materials to fine-tune performance, workability, and durability for specific applications.[5,6] These empirical additions were based on local knowledge and available resources. Various organic additives and admixtures were incorporated into lime mortars to enhance properties such as ductility, adhesion, mechanical and weather resistance, and to slow down the setting time. Common organic additives included animal-based additives such as eggs (particularly egg white), milk, casein, gelatine, and fish glue, which improved cohesion and strength of the mortar.[7,8] For example, the construction mortars in the Forbidden City built by Ming and Qing dynasties in Beijing, China, contained casein, collagen, ovalbumin, blood and protein.[9] Other additives were based on plants, including starches (*e.g.*, wheat or potato starch), glucose, gum arabic, cellulose, and bird guano or plant extracts, which enhanced workability and adhesion.[10] Straw, hemp fibres, wood shavings, or sawdust, served as reinforcement to reduce cracking during drying and mechanical loading.[11] Natural oils and resins like linseed oil, tar, resin, and pitch were used to increase water resistance and resistance to cracking under mechanical stress.[12,13] These organic additives, admixtures and fibres were typically selected based on local availability and traditional knowledge, resulting in each historic mortar having unique characteristics tailored to specific climatic conditions and building requirements.

[a] *Department of Materials Engineering and Chemistry, Faculty of Civil Engineering, Czech Technical University in Prague, Prague, Czech Republic.*
E-mail: pavlikz@fsv.cvut.cz, adam.pivak@fsv.cvut.cz, martina.zaleska@fsv.cvut.cz, milena.pavlikova@fsv.cvut.cz
[b] *Department of Water Supply and Wastewater Disposal, Faculty of Environmental Engineering and Energy, Lublin University of Technology, Lublin, Poland.*
E-mail: g.lagod@pollub.pl
[c] *Department of Inorganic Chemistry, Faculty of Chemical Technology, University of Chemistry and Technology, Prague, Czech Republic.*
E-mail: ondrej.jankovsky@vscht.cz

Nowadays, the use of materials similar to those employed historically prevails in modern conservation practice, and extensive research focuses on historically well-documented natural materials to produce repair mortars. Current trends are driven by two key aspects: (i) the development of materials that are compatible with historic structures, and (ii) the sustainability of their production, which is closely linked to both economic and environmental benefits. Brzyski *et al.*[14] used gum arabic (GA) as a sustainable modifier for lime–metakaolin mortars. GA increased the water retention capacity of the fresh mortar and reduced its drying shrinkage. In hardened mortars, higher GA dosages decreased water absorption and total porosity, while significantly improving both flexural and compressive strength. The addition of sticky rice to lime mortar was found to enhance its elasticity through interactions with calcium carbonate crystals.[15] Bilwa fruit extract was positively influenced both the compressive and flexural strength of hydraulic lime mortars.[16] Gour *et al.*[17] observed that incorporating areca nut extract as an additive improved both the fresh and hardened performance of air-lime mortars. Likewise, Ravi *et al.*[18] showed that cactus extract contributed to enhanced mechanical strength and durability in NHL-based mortars. Reinforcement of lime mortars with natural fibres which are abundant, low-cost, sustainable, energy efficient, non-toxic and biodegradable represents popular technique to improve performance of mortars for repair of historic masonry.[19,20]

To contribute to current trends in the repair and conservation of historic buildings, including those listed as heritage sites, and to adhere to the principles of compatibility and sustainability in designing alternative mortars, this research evaluates the effect of mechanically processed eggshells as a partial substitute for silica sand in mortars intended for historic building repairs. In addition, the workability of the fresh mortars is maintained by using egg white as a natural modifying agent. Because the use of eggshell powder in construction mortars has been rarely studied,[21] this issue requires more comprehensive investigation and analysis. One of the few studies on eggshell powder was conducted by Sivakumar and Mahendran,[22] who examined the strength and permeability of concrete incorporating fly ash, rice husk ash, and eggshell powder. Their results showed improvements in these properties through an optimal combination of these mineral admixtures as part of a blended cement. Recently, Nandhini and Sundar[23] investigated the use of eggshell powder as a partial substitute for cement in ''greener'' mortars. Similarly, Nandhini and Karthikeyan[24,25] dried, ground, and calcined eggshells and applied them as a cementitious material in concrete production. The authors also reported a micro-filling effect of the eggshell powder, contributing to densification of the hardened matrix. Nevertheless, to the best of the authors' knowledge, no studies have addressed the use of non-calcined fine eggshell powder in lime-based mortar compositions compatible with the repair and restoration of historic buildings, which underlines the novelty of the research presented herein. The intention of the investigation was to use eggshells without any additional energy-demanding processing, such as calcination, which is commonly applied in previous studies. Calcination typically requires temperatures exceeding 800–900 °C and is therefore associated with high energy consumption and additional CO_2 emissions. By deliberately avoiding this thermal treatment and employing exclusively mechanical processing, the proposed approach significantly reduces the environmental footprint of eggshell valorisation and enables a low-energy, sustainable reuse of an abundant bio-waste material in lime-based mortars.

Moreover, the increasing volume of eggshell residues generated by intensive poultry farming and food-processing activities represents a growing challenge for contemporary waste management practices. In many cases, eggshell waste is disposed of in landfills, where it occupies valuable landfill capacity and can lead to the formation of methane as residual organic components decompose under oxygen-deficient conditions. Given that methane has a substantially higher global warming potential than carbon dioxide, such emissions contribute disproportionately to climate change. Moreover, the breakdown of eggshell waste may produce leachates capable of adversely affecting surrounding soil and groundwater systems. Consequently, the development of environmentally responsible and value-added uses for eggshell waste has become an important priority from both sustainability and regulatory standpoints.

Materials and methods

The present experimental investigation focused on analysing the effects of mechanically treated eggshells and egg white on the properties and performance of lime mortars. The study includes characterization of mechanically processed eggshells used as a partial replacement for silica sand, the design and preparation of mortar mixtures, and testing of samples cured for 28 and 90 days. Attention was given to evaluating the impact of egg-shells on the mechanical strength, hygric behaviour, and thermal performance of the specimens. The results were compared against the limits and recommended values specified by the WTA International guidelines (WTA Recommendation 2-9-04 ''Systems of Protective/Renovation Renderings''[26]) and EN 998-1 standards.[27] The flow chart of the conducted research is presented in Fig. 1.

Materials and sample preparation

The mortars for testing were prepared using hydrated lime CL90-S (Čertovy schody s.r.o., Lhoist Group, Czech Republic). For the reference mortar (LM-REF), silica sand (Filtrační písky, Ltd, Chlum, Czech Republic) in three particle-size fractions was used as the sole aggregate.

These fractions were designated PG1 (0–0.5 mm), PG2 (0.5–1 mm) and PG3 (1–2 mm), and were combined at a mass ratio of 1 : 1 : 1. In the reference mixture, the binder-to-filler ratio was 1 : 3 by mass. Water was added to all mixtures at a water-to-binder mass ratio of 1 : 1. To prepare the modified mortars, part of the PG1 fraction was replaced with eggshells pre-ground in a ball mill, at volumetric replacement levels of

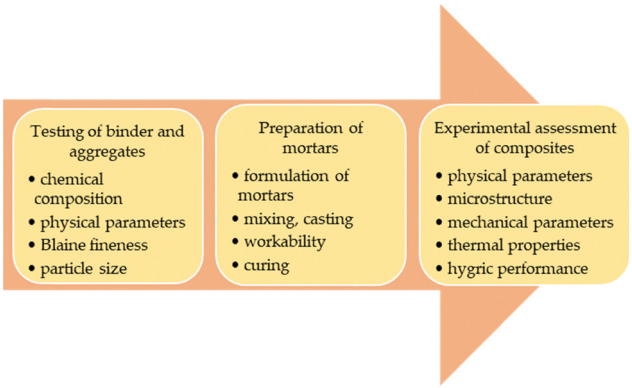

Fig. 1 Flow chart of conducted research.

25%, 50%, and 75%. These mixtures were marked LM-ES-25, LM-ES-50 and LM-ES-75. The raw eggshells and the eggshell powder are shown in Fig. 2. The spread diameter, as determined by a flow table test, was adjusted to 165 ± 5 mm for all mortars. To achieve the required workability, egg white (Eurovo Pro Up, France) was added to the modified mixtures. The formulations of the mortars are presented in Table 1, with the contents of all components expressed in grams (g). The mixing was conducted using a planetary mixer (ELE International, Milton Keynes, UK) and followed the procedures outlined in EN 459-2.[28] Fresh mortar was poured into moulds of various shapes and sizes. These included prismatic moulds measuring 40 × 40 × 160 mm, cubic moulds with 40 mm sides, and cylindrical discs with a diameter of 100 mm and a height of 20 mm. The mixtures were then left to harden for 72 hours. During this period, the specimens were covered with plastic foil to minimise moisture loss and reduce the likelihood of shrinkage-induced cracking. After demoulding, the specimens continued to cure for two different durations – for a total of 28 and 90 days under controlled environmental conditions in climatic chamber, with relative humidity maintained at 90% ± 5% and temperature held at 23 °C ± 2 °C. The samples prepared for testing shows Fig. 3.

Characterization of lime hydrate, processed eggshells and silica sand

The loose bulk density of all input materials was determined using the gravimetric method. The specific gravity was measured by helium pycnometry with a Pycnomatic ATC apparatus (Thermo Scientific™). The specific surface area was obtained by an air permeability test using a Blaine UTCM-0280 automatic device (UTEST). The chemical composition of lime hydrate, milled eggshells, and silica sand was analysed with an ARL Quant'X EDXRF spectrophotometer (Thermo Scientific™).

The mineralogical composition of eggshells was determined by X-ray diffraction using (XRD) a D2 Phaser diffractometer (Bruker). The morphology of the milled eggshell particles was examined by scanning electron microscopy SEM (Lyra dual-beam, Tescan), and their surface chemical composition was analysed by energy-dispersive spectroscopy EDS (X-MaxN, Oxford Instruments).

Two different methods were applied to assess particle size distribution, selected ac-cording to the maximum particle size of each material. The particle size of lime hydrate and eggshell powder was measured by laser diffraction using an Analyssette 22 Micro Tec plus (FRITSCH). For silica sand, particle size distribution was determined by sieving in accordance with EN 1015-1.[29]

Methods of testing fresh and hardened mortars

The workability of the fresh mortars was assessed by measuring the spread diameter in accordance with EN 1015-3.[30] Besides mechanical and macro-structural properties, the testing programme included MIP analysis, evaluation of thermal conductivity and heat storage parameters, and assessment of hygric characteristics of hardened mortars. Except MIP test and measurement of sorption isotherms, the experimental analyses

Table 1 Formulation of mortar mixtures (g)

Mortar mix	Lime hydrate	PG1	PG2	PG3	Eggshells	Water	Egg white
LM-REF	2650	2650	2650	2650	—	2650	—
LM-ES-25	2650	1987.5	2650	2650	396.8	2650	610
LM-ES-50	2650	1325	2650	2650	793.6	2650	767
LM-ES-75	2650	662.5	2650	2650	1190.4	2650	787

Fig. 3 Prismatic specimens of lime mortars, from left: LM-REF, LM-ES-25, LM-ES-50, LM-ES-75.

Fig. 2 Raw and mechanically processed eggshells.

were carried out for both curing regimes, *i.e.* for 28-day and 90-day samples.

The basic structural characteristics of mortars were determined on specimens dried in a vacuum chamber at 60 °C until constant mass was achieved. The measured properties included bulk density (ρ_b), specific density (ρ_s), and open porosity (φ). Bulk density was determined gravimetrically according to EN 1015-10,[31] while specific density was measured pycnometrically. Open porosity was calculated using the measured bulk and specific density values. In addition, the 90-day samples underwent detailed pore structure characterisation by mercury intrusion porosimetry (MIP) using Pascal MIP 140 and 440 (Thermo Scientific™) modules.

Mechanical strength was determined according to EN 1015-11[32] using a FP 100 mechanical press (Heckert). Flexural strength was measured in a three-point bending test on 40 mm × 40 mm × 160 mm prisms with a support span of 100 mm. The resulting fragments were then used for compressive strength testing, performed on a 40 mm × 40 mm loading area. Young's modulus was calculated from ultrasonic pulse velocity measurements in accordance with EN 12504-4,[33] using a Vikasonic ultrasonic testing device (Schleibinger Geräte). Before testing, specimens were dried in a vacuum chamber to eliminate the influence of moisture on measurement accuracy.

The thermal properties examined included dry thermal conductivity and volumetric heat capacity, measured using an ISOMET 2114 device (Applied Precision). Capillary water absorption test[34,35] was used to determine the water absorption coefficient and apparent moisture diffusivity. Water absorption was measured in 3D suction experiment. Sorption isotherms of the 90-day mortars were obtained using the absorption method. Water vapour transmission parameters were measured using the cup method in accordance with EN ISO 12572.[36] Fig. 4 schematically illustrates the preparation and testing of the specimens. The measurement uncertainties of the applied test methods, along with further details, are presented in a previous publication.[37]

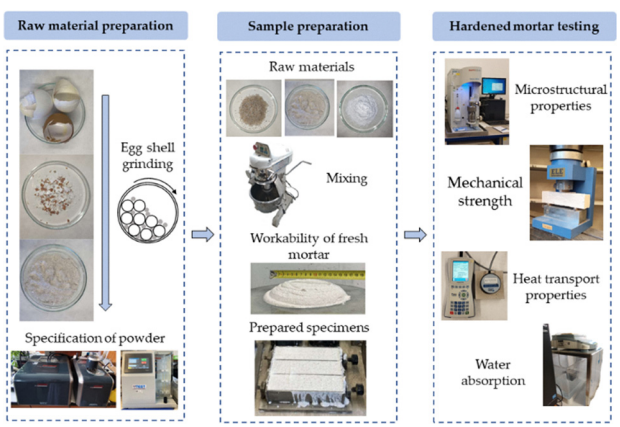

Fig. 4 Preparation of specimens and their testing.

Results

Characterisation of raw materials

Both the lime hydrate and the eggshell powder exhibited similar chemical compositions, with CaO identified as the predominant oxide. Al_2O_3 and MgO were pre-sent as additional major constituents. The presence of SO_3 in the eggshell powder (0.33 wt%) can be explained mainly by trace sulphur contained in the organic fraction of the shells. In addition, minor amounts of sulphates may originate from the hen's diet or from processing and handling, which can also contribute to the detected SO_3. For the aggregate, SiO_2 was confirmed as the principal component of the silica sand, with Al_2O_3 also detected in smaller amounts. The main chemical composition (expressed as oxides) of the raw materials are summarised in Table 2.

The fundamental physical parameters of the tested raw materials are presented in Table 3. The loose bulk density of eggshell powder is significantly lower compared to all fractions of silica sand. Consequently, an increase in eggshell powder dosage, *i.e.*, a higher substitution level of PG1, can be expected to lighten the mortars. The Blaine specific surface area of lime hydrate contributes to its high reactivity. Additionally, the hierarchical structure[38] and porosity[39] of eggshells result in a high specific surface area and complex morphology.

The morphological properties of the particles of mechanically processed eggshells are well seen in the SEM micrographs as shown in Fig. 5 at different magnifications. As the particles were mechanically ground, they are shown to have irregular shape having a complex hierarchical and layered structure with tabular and prismatic calcite crystals.

Table 2 Chemical composition of lime hydrate, eggshells, and silica aggregate used

Material	Lime hydrate	Eggshell powder	Sand
CaO	95.56	93.44	0.01
Al_2O_3	3.00	3.34	3.14
SiO_2	0.21	0.18	96.30
MgO	1.10	1.97	0.37
Fe_2O_3	0.07	0.02	0.04
SrO	0.04	0.05	—
NiO	0.02	0.01	—
Na_2O	—	—	—
K_2O	—	—	0.02
SO_3	—	0.33	0.01
MnO	—	—	—
TiO_2	—	—	0.11
P_2O_5	—	0.51	—
Σ	100.00	100.00	100.00

Table 3 Physical properties of raw materials used

Material	Loose bulk density (kg m^{-3})	Specific density (kg m^{-3})	Blaine specific surface (m^2 kg^{-1})
Lime Hydrate	446	2230	1657
Eggshell powder	837	2457	987
Silica sand PG1	1397	2662	—
Silica sand PG2	1435	2666	—
Silica sand PG3	1463	2665	—

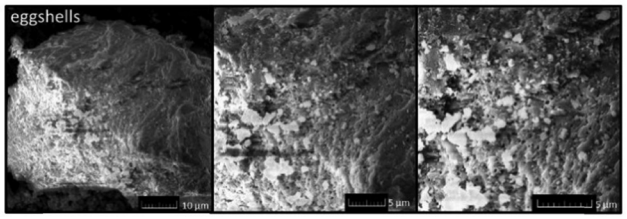

Fig. 5 SEM scans of eggshell particle.

The X-ray diffraction patterns of eggshells shows Fig. 6. The prevailing crystalline phase identified was $CaCO_3$ which well agrees with XRF data and those previously published.[23–25] Although eggshells are composed mainly of calcite, trace amounts of phosphorus-containing phase ($CaHPO_4$) were detected which is commonly attributed to the presence of shell membranes or minor inorganic impurities.

Fig. 7 shows the elemental distribution in eggshell powder as determined by EDS analysis. The main elements correspond to those found by XRF and are evenly distributed throughout the sample. Contrary to XRF data, EDS evinced the presence of Na and Cl. The trace amount of these elements is typically incorporated into the eggshell during its formation as the results of hens' diet and metabolism. No clusters or localised concentrations of the elements identified were detected.

Particle size distributions of the binder, eggshell powder, and the finest fraction of silica sand (PG1) were determined using laser diffraction analysis. The particle size distribution curves, both cumulative and incremental, are shown in Fig. 8,

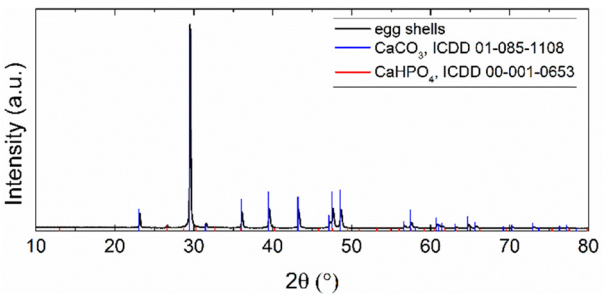

Fig. 6 X-ray diffraction patterns of eggshells.

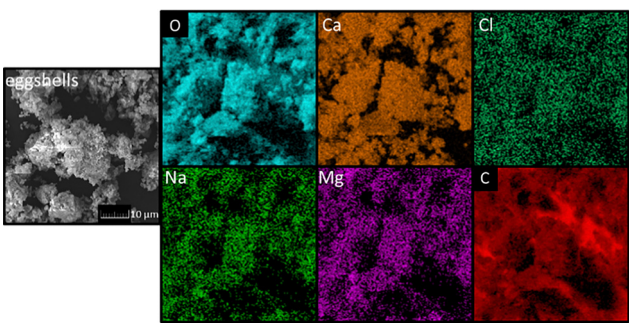

Fig. 7 Elemental mapping of eggshell particles.

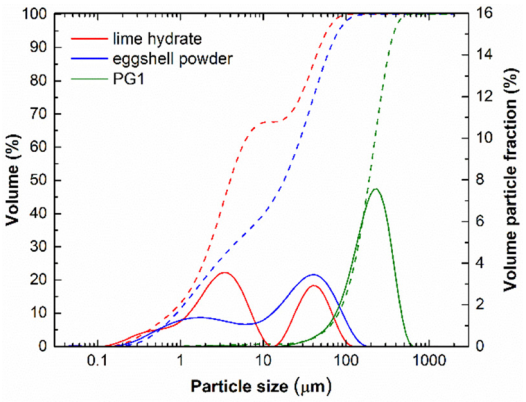

Fig. 8 Particle size distribution of lime hydrate, eggshell powder and fraction PG1 of silica sand.

while the key parameters $d90$, $d50$, and $d10$ are summarized in Table 4. Consistent with the Blaine specific surface data, lime hydrate was the finest material analysed. Eggshell powder was coarser than lime hydrate but significantly finer than the sand fraction PG1. Unlike eggshell powder, PG1 contained no "dust" particles smaller than 10 µm. Furthermore, the incremental particle size distribution curves of both lime hydrate and eggshell powder exhibited a bimodal pattern, whereas PG1 showed a unimodal distribution.

The granulometry curve of the silica sand shows Fig. 9 and apparently corresponds to the grading of the delivered sand fractions.

Table 4 The particle size distribution parameters of lime hydrate, eggshell powder and sand

Material	d_{10} (µm)	d_{50} (µm)	d_{90} (µm)
Lime hydrate	0.8	4.3	51.4
Eggshell powder	0.9	18.8	68.4
Silica sand PG1	76.2	192.4	348.3

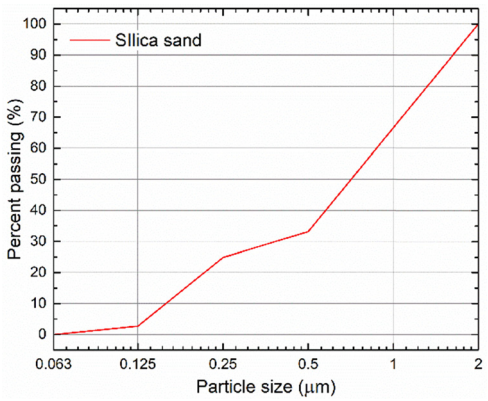

Fig. 9 Granulometry curve of silica aggregate.

Table 5 Macrostructural parameters of 28-day and 90-day mortars

	ρ_b (kg m^{-3})		ρ_s (kg m^{-3})		φ (%)	
Mortar type	28 days	90 days	28 days	90 days	28 days	90 days
LM-REF	1665 ± 23	1694 ± 24	2550 ± 31	2534 ± 30	34.7 ± 0.7	33.1 ± 0.7
LM-ES-25	1539 ± 22	1540 ± 22	2532 ± 30	2529 ± 30	39.2 ± 0.8	39.1 ± 0.8
LM-ES-50	1488 ± 21	1529 ± 21	2512 ± 30	2517 ± 30	40.8 ± 0.8	39.2 ± 0.8
LM-ES-75	1405 ± 20	1435 ± 20	2518 ± 30	2499 ± 30	44.6 ± 0.9	42.9 ± 0.9

Testing of hardened mortars

Several distinctive features were distinguished based on the analysis of acquired fundamental macrostructural properties. Bulk density greatly reduced with the increasing dosage of eggshell powder in composition of mortars, *i.e.*, with the substitution rate of silica aggregate by milled eggshells. Similarly, the specific density was lowered by the incorporation of eggshell powder in mortar mixes. On the contrary, with the dropped bulk density and specific density, the porosity of mortars was enhanced, which is positive regarding to assumed use of the modified mortars in repair and conservation works. Taking into consideration the criteria imposed on repair mortars by WTA International guidelines,[26] the mortars labelled LM-ES-50 and LM-ES-75 met the criteria on porosity value and LM-ES-75 even on the bulk density value. The investigated macrostructural characteristics varied in time, *i.e.* the porosity was reduced due to the continuous carbonation of mortars, which well correlated with the in-creased bulk density. The fundamental macrostructural properties of hardened mortars are shown in Table 5. For the 90-day samples, the pore size distribution was evaluated using MIP. The cumulative and incremental pore size distribution curves are shown in Fig. 10 and 11. The microstructural parameters derived from these curves are summarized in Table 6.

The total pore volume followed the same trend as the porosity data presented in Table 5; *i.e.*, the highest total pore volume was observed for mortar LM-ES-75, while the reference mortar LM-REF exhibited the lowest value. The coarsening of the pore structure resulting from the partial substitution of silica sand fraction PG1 with eggshell powder is well evidenced by the average pore diameter and by the incremental pore size distribution curves in Fig. 7, where a clear shift of the pore diameter first peak from approximately 0.34 μm to about 1.0 μm can be observed.

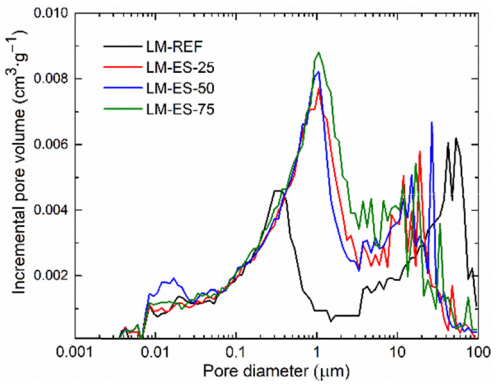

Fig. 10 Pore size distribution of 90-day samples – incremental curves.

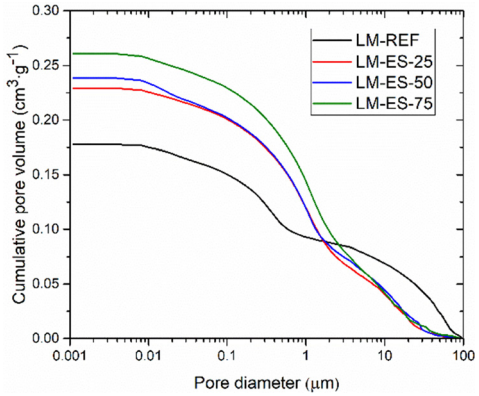

Fig. 11 Pore size distribution of 90-day samples – cumulative curves.

Table 6 Microstructural characteristics of 90-day mortars obtained by MIP

Mortar type	Total pore volume V_t (cm^3 g^{-1})	Average pore diameter d_a (μm)
LM-REF	0.1789	0.1111
LM-ES-25	0.2298	0.1256
LM-ES-50	0.2390	0.1273
LM-ES-75	0.2612	0.1286

Compressive and flexural strength results are shown in Fig. 12 and 13. Quantitatively, the obtained values are consistent with those reported in the RILEM TC 277-LHS report – Lime-based mortars for restoration – a review on long-term durability aspects and experience from practice.[40] Owing to the slow hardening mechanism of the binder (carbonation), and in agreement with the gradual decrease in porosity over time, both mechanical parameters improved with prolonged curing, which is favourable for their practical application in conservation practice. The highest mechanical strength was achieved by the reference mortar LM-REF, whereas a noticeable reduction in mechanical performance was observed for the modified mortars, with the decline further amplified by increasing the eggshell content. For the 90-day samples, the compressive strength de-creased by 14.3%, 28.8%, and 38.1% for LM-ES-25, LM-ES-50, and LM-ES-75, respectively.

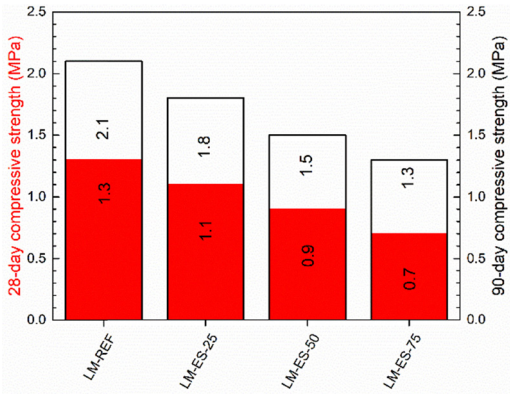

Fig. 12 Compressive strength of hardened mortars.

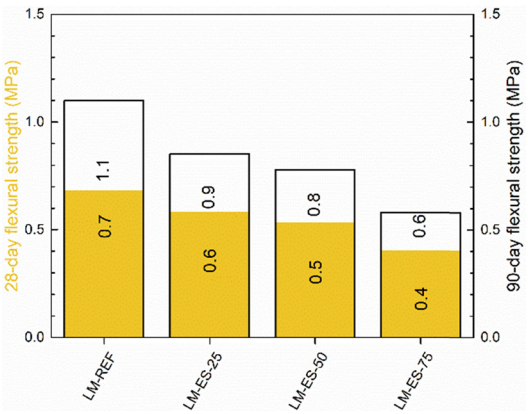

Fig. 13 Flexural strength of hardened mortars.

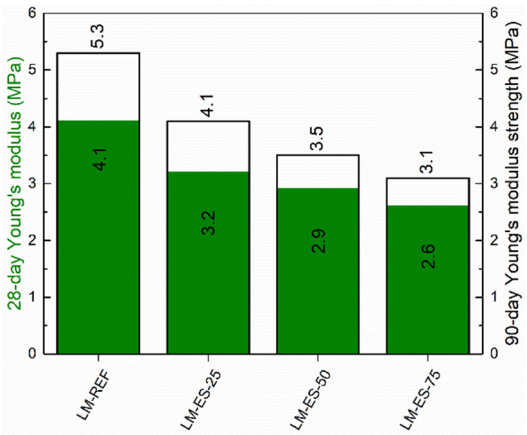

Fig. 14 Dynamic modulus of elasticity of the hardened mortars.

Table 7 Water transport parameters of 90-days samples

Mortar	Water absorption coefficient $\times 10^{-2}$ (kg m^{-2} s$^{-1/2}$)	Moisture diffusivity $\times 10^{-7}$ (m^2 s^{-1})	Water absorption (kg m^{-3})
LM-REF	28.6 ± 0.7	10.8 ± 0.2	275.9 ± 3.9
LM-ES-25	23.1 ± 0.5	5.37 ± 0.1	315.9 ± 4.4
LM-ES-50	19.5 ± 0.4	3.64 ± 0.1	320.5 ± 4.5
LM-ES-75	16.7 ± 0.4	2.76 ± 0.1	323.7 ± 4.5

According to the WTA International guidelines,[26] suitable repair mortars should exhibit compressive strength in the range of 1.5–5.0 MPa. All mortars investigated complied with this requirement, with the exception of LM-ES-75, whose compressive strength was slightly below the lower WTA limit. However, it should be noted that several authors recommend considerably lower compressive strength values for lime-based repair mortars, typically in the range of 0.5–1.5 MPa, in order to ensure compatibility with historic masonry substrates.[5,41,42] In this context, the compressive strength of LM-ES-75 falls within the broader, literature-suggested range for restoration mortars. Similarly, Nogueira *et al.*[43] proposed technical criteria for replacement rendering mortars with 90-day compressive strength between 0.4 and 2.5 MPa, in agreement with the recommendations of Silva *et al.*[44]

All studied mixes showed a low compressive-to-flexural strength ratio, indicating elastic behaviour compatible with repair applications.[45] The WTA sets the upper limit for this ratio at < 3, which all mortars comfortably satisfied. The low fc/ff ratio also reflects a low modulus of elasticity, presented in Fig. 14. Water transport parameters of the 90-day samples are summarized in Table 7.

Although the incorporation of eggshell powder into the mortar composition increased both porosity and average pore size, the ingress of liquid water was significantly slowed, as clearly demonstrated by the water absorption coefficient and apparent moisture diffusivity data.

In a preliminary study investigating lime-based mortars with egg white addition, Zhang *et al.*[46] reported that egg white reduces water absorption, thereby enhancing water resistance. It is therefore anticipated that denatured proteins in the egg white orient themselves along the pore surfaces, with their hydrophobic segments facing outward. As a result, a partially hydrophobic pore surface is formed, leading to reduced capillary water absorption. However, since water absorption was measured using a 3D suction experiment, the overall reduction in pore capillarity was offset, and the measured values correlated with porosity and other microstructural characteristics.

The ability to transport water vapor was characterized by the water vapor diffusion resistance factor (Table 8), with the WTA International setting the limit at less than 12.[26] Based on the results of the cup test, it was found that the vapor diffusion resistance factor decreased with the addition of eggshell powder in the mortar composition, and the water vapor transmission capability improved as the dosage of eggshell powder increased. Furthermore, all LM-ES mortars met the WTA criterion, enabling the treated masonry to ''breathe'' and effectively dry out.

The parameters describing heat transfer and storage are presented in Table 9. The thermal conductivity values correspond to the changes in porosity resulting from the incorporation of ground eggshells into the plaster mixtures as a partial replacement for fine sand, as well as to the significantly

Table 8 Water vapor diffusion resistance factor of 90-day samples

Mortar	Water vapor resistance factor μ_d – dry cup test (–)	Water vapor resistance factor μ_w – wet cup test (–)
LM-REF	12.2 ± 0.3	11.2 ± 0.3
LM-ES-25	11.8 ± 0.3	9.8 ± 0.2
LM-ES-50	11.3 ± 0.3	8.7 ± 0.2
LM-ES-75	10.9 ± 0.3	8.1 ± 0.2

Table 9 Thermal characteristics of hardened mortars

Mortar	Thermal conductivity λ (W m^{-1} K^{-1})	Volumetric heat capacity $C_v \times 10^6$ (J m^{-3} K^{-1})
LM-REF	1.125 ± 0.026	1.490 ± 0.034
LM-ES-25	0.919 ± 0.021	1.523 ± 0.035
LM-ES-50	0.777 ± 0.179	1.580 ± 0.036
LM-ES-75	0.707 ± 0.016	1.501 ± 0.035

lower bulk density of eggshells compared to quartz sand. Quantitatively, the thermal parameters of the studied lime plasters are consistent with the results reported by Pivák *et al.*[47]

Although the thermal conductivity decreased by up to 37.2% for LM-ES-75, the mortar still cannot be classified as a thermal insulation mortar. However, it should be noted that current standards do not impose any thermal-performance requirements on repair mortars.

Sorption and desorption isotherms of 90-day mortars are shown in Fig. 15. The combination of eggshell powder and egg white significantly reduced the maximum moisture content stored within the porous structure of LM-ES mortars. Two competing mechanisms influenced water vapor storage: the increased porosity caused by partial re-placement of PG1 with eggshell powder, and the hydrophobic effect of proteins in the egg white, which form a hydrophobic layer on the pore surfaces. Quantitatively, the moisture content stored in LM-ES mortars was low, with maximum values at 98.0% RH of 1.3 wt%, 1.1 wt%, and 0.8 wt% for LM-ES-50, LM-ES-75, and LM-ES-25, respectively. The residual moisture remaining in the samples after completing the desorption cycles was negligible

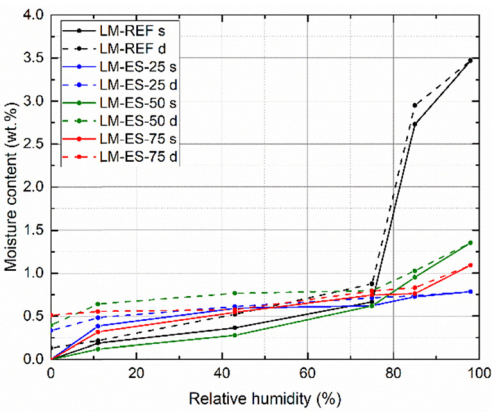

Fig. 15 Sorption and desorption isotherms of 90-day mortars.

in terms of mortar performance and durability, ranging between 0.1 and 0.5 wt%.

Conclusion

The presented research contributes to current trends in the conservation and repair of historic building stock by developing compatible lime-based mortars. The design of these mortars also addresses sustainability concerns by partially substituting the finest silica sand with mechanically processed eggshell powder and incorporating egg white as both a workability agent and a modifier of the mortars' hygric properties and other water-related performance. Based on the comprehensive experimental data obtained, the following key findings can be highlighted:

- the addition of eggshell powder increased the porosity of the mortars, achieving values compliant with WTA International guidelines for repair mortars;
- both total pore volume and average pore diameter increased with higher dosages of eggshell powder;
- the LM-ES mortars maintained adequate mechanical strength suitable for repair applications;
- water ingress and transport were significantly reduced due to denatured proteins in egg white forming hydrophobic segments on the pore surfaces;
- water vapour transmission capability improved with increasing dosage of eggshell powder, indicating the enhanced "breathability" of the mortars;
- water vapour storage determined from sorption/desorption isotherms was reduced relative to the reference mortar, due to partial hydrophobicity of the pore surfaces;
- the thermal insulation function of mortars with eggshell powder was much better than identified for reference mortar;
- the reduced capillary water absorption suggests improved resistance to moisture-related deterioration.

From a sustainability perspective, the use of non-calcined eggshell powder is particularly advantageous, as it avoids energy-intensive thermal treatment typically associated with calcination and the related CO_2 emissions. The proposed approach thus enables direct, low-energy valorisation of eggshell waste through purely mechanical processing, contributing to reduced environmental impact and alignment with circular economy principles.

However, it should be noted that these results are preliminary, focusing on the effects of egg-shell powder and egg white on lime-based mortars. Further research is necessary, with planned studies to investigate the durability of these mortars and their adhesion to various substrate types.

Author contributions

Conceptualization, Z. P.; methodology, Z. P., M. P. and O. J.; formal analysis, Z. P., A. P., M. Z., M. P. and O. J.; investigation, A. P., M. Z., G. Ł. and M. P.; data curation, Z. P. and M. P.; writing – original draft preparation, Z. P., M. Z., M. P., G. Ł. and

O. J.; writing – review and editing, Z. P., M. P. and O. J.; supervision, Z. P., M. P. and O. J.; project administration, G. Ł. and M. P.; funding acquisition, Z. P. and O. J. All authors have read and agreed to the published version of the manuscript.

Conflicts of interest

There are no conflicts to declare.

Data availability

According to Open Science principes data can be found at https://doi.org/10.5281/zenodo.17950740.

Acknowledgements

This research was funded by CZECH SCIENCE FOUNDATION, grant number 25-15998S, while the infrastructure has been utilized in the frame of project no. CZ.02.01.01/00/22_008/0004631 Materials and technologies for sustainable development within the Jan Amos Komensky Operational Program financed by the European Union and from the state budget of the Czech Republic. The work carried out at the Lublin University of Technology was supported by the Polish Ministry of Education and Science within the individual grant of scientific discipline Environmental Engineering, Mining and Energy.

References

1 M. Doğruyol, *Case Stud. Constr. Mater.*, 2024, **21**, e03542.
2 M. Pavlíkova, L. Zemanová, M. Záleská, J. Pokorný, M. Lojka, O. Jankovský and Z. Pavlík, *Materials*, 2019, **12**(6), 996.
3 M. R. Veiga, A. Fragata, A. L. Velosa, A. C. Magalhães and G. Margalha, *Int. J. Archit. Herit.*, 2010, **4**(2), 177–195.
4 B. A. Silva, E. Guerreiro and A. P. C. Duarte, *Constr. Build. Mater.*, 2025, **499**, 143956.
5 J. Elsen, *Cem. Concr. Res.*, 2006, **36**, 1416–1424.
6 P. Pizzo, J. Válek and D. Frankeová, *J. Archeol. Sci. Rep.*, 2025, **65**, 105235.
7 L. Rampazzi, M. P. Colombini, C. Conti, A. Luveras-Tenorio, A. Sansoneti and M. Zanaboni, *Archaometry*, 2015, **58**(1), 115–130.
8 K. Zhang, L. Rampazzi, M. P. Riccardi, A. Sansonetti and A. Grimoldi, *Adv. Geosci.*, 2018, **45**, 19–24.
9 K. Zhai, H. Zhu, L. Luo, B. Zhang, L. Zhu, Q. Zhang and P. Zhao, *J. Cult. Herit.*, 2024, **70**, 71–79.
10 E. Gliozzo, A. Pizzo and M. F. La Russa, *Arch. Anthrop. Sci.*, 2021, **13**, 193.
11 F. Kesikidou and M. Stefanidou, *J. Build. Eng.*, 2019, **25**, 100786.
12 K. Saggu, S. Pal and N. Dev, *J. Cult. Herit.*, 2025, **76**, 317–326.
13 Z. Zhang, B. Zhang, Y. Hu and Z. Wang, *J. Archeol. Sci.*, 2025, **175**, 106149.
14 P. Brzyski, M. Matejdes, I. Medved and M. Slaný, *Constr. Build. Mater.*, 2025, **493**, 143146.
15 Y. Zeng, B. Zhang and X. Liang, *Thermochim. Acta*, 2008, **473**, 1–6.
16 D. Shanmugavel, R. Dubey and R. Ramadoss, *J. Build. Eng.*, 2020, **30**, 101252.
17 K. A. Gour, R. Ravi and S. Thirumalini, *Constr. Build. Mater.*, 2018, **164**, 255–264.
18 R. Ravi, S. Thirumalini and S. K. Sekar, *Int. J. Architect. Herit.*, 2016, **10**, 714–725.
19 C. Giosuè, A. Mobili, Q. L. Yu, H. J. Brouwers, M. L. Ruello and F. Tittarelli, *J. Sustainable Cem.-Based Mater.*, 2019, **8**(4), 214–227.
20 M. Stefanidou, V. Kamperidou, A. Konstantinidis, P. Koltsou and S. Papadopoulos, *Constr. Build. Mater.*, 2021, **298**, 123881.
21 H. Binici, O. Aksogan, A. H. Sevinc and E. Cinpolat, *Constr. Build. Mater.*, 2015, **93**, 1145–1150.
22 M. Sivakumar and N. Mahendran, *J. Theor. Appl. Inform. Technol.*, 2014, **66**, 489–499.
23 K. Nandhini and M. S. S. Sundar, *Cleaner Waste Systems*, 2025, **12**, 100408.
24 K. Nandhini and J. Karthikeyan, *Constr. Build. Mater.*, 2022, **335**, 127482.
25 K. Nandhini and J. Karthikeyan, *Mater. Sci. Forum*, 2022, **1053**, 323–330.
26 WTA International e.V., WTA Recommendation 2-9-04; Systems of Protective/Renovation Renderings, 2004.
27 CEN, EN 998-1; Specification for mortar for masonry – Part 1: Rendering and plastering mortar., 2016.
28 CEN, EN 459-2; Building lime-Part 2: Test Methods., 2021.
29 CEN, EN 1015-1; Methods of Test for Mortar for Masonry-Part 1: Determination of Particle Size Distribution (by Sieve Analysis)., 1999.
30 CEN, EN 1015-3; Methods of Test for Mortar for Masonry-Part 3: Determination of Consistence of Fresh Mortar (by Flow Table)., 2000.
31 CEN, EN 1015-10; Methods of Test for Mortar for Masonry—Part 10: Determination of Dry Bulk Density of Hardened Mortar., 2000.
32 CEN, EN 1015-11; Methods of Test for Mortar for Masonry—Part 11: Determination of Flexural and Compressive Strength of Hardened Mortar., 2020.
33 CEN, EN 12504-4; Testing Concrete in Structures—Part 4: Determination of Ultrasonic Pulse Velocity, 2021.
34 CEN, EN 1015-18; Methods of Test for Mortar for Masonry—Part 18: Determination of Water Absorption Coefficient Due to Capillarity Action of Hardened Mortar., 2003.
35 Z. Pavlík and R. Černý, *Int. J. Thermophys.*, 2012, **33**, 1704–1714.
36 ISO, EN ISO 12572; Hygrothermal performance of building materials and products – Determination of water vapour transmission properties – Cup method., 2016.
37 Z. Pavlík, M. Vyšvařil, M. Pavlíková, T. Žižlavský, M. Záleská and A. Pivák, *J. Build. Eng.*, 2023, **79**, 107841.

38 D. Athanasiadou, W. Jiang, D. Goldbraum, A. Saleem, K. Basu, M. S. Pacella, M. S. Bohm, R. R. Chromik, M. T. Hincke, A. B. Rodriguéz-Navarro, H. Vali, S. E. Wolf, J. J. Gray, K. H. Bui and M. D. McKee, *Sci. Adv.*, 2018, **4**(3), eaar3219.
39 I. Arzate-Vázquez, J. V. Méndez-Méndez, E. A. Flores-Johnson, J. Nicolás-Bermúdez, J. J. Chanona-Pérez and E. Santiago-Cortés, *Micron*, 2019, **118**, 50–57.
40 C. Groot, R. Veiga, I. Papayianni, R. Van Hees, M. Secco, J. I. Alvarey, P. Faria and M. Stefanidou, *Mater. Struct.*, 2022, **55**, 245.
41 G. Borsoi, A. Santos Silva, P. Menezes, A. Candeias and J. Mirão, *Constr. Build. Mater.*, 2019, **204**, 597–608.
42 D. Barnat-Hunek, M. Gryegorczyk-Franczak, B. Klimek, M. Pavlíková and Z. Pavlik, *Constr. Build. Mater.*, 2021, **278**, 122366.
43 R. Nogueira, A. P. F. Pinto and A. Gomes, *Cem. Concr. Compos.*, 2018, **89**, 192–204.
44 B. A. Silva, A. P. F. Pinto and A. Gomes, *Constr. Build. Mater.*, 2015, **94**, 346–360.
45 A. Maropoulou, A. Bakolas, P. Moundoulas, E. Aggelakopoulou and S. Ananostoupoulou, *Cem. Concr. Compos.*, 2005, **27**(2), 289–294.
46 K. Zhang, L. Wang, F. Tie, F. Yang, Y. Liu and Y. Zhang, *Int. J. Architect. Herit.*, 2020, **16**, 1184–1198.
47 A. Pivák, M. Záleská, M. Pavlíková and Z. Pavlík, *J. Compos. Sci.*, 2025, **9**, 266.